Electrical Power and Energy Systems 60 (2014) 389–398

Contents lists available at ScienceDirect

Electrical Power and Energy Systems

journal homepage: www.elsevier.com/locate/ijepes

Optimal placement and sizing of distributed generators based on a novel MPSI index

Ruhaizad Ishak [a,b,*], Azah Mohamed [a], Ahmed N. Abdalla [b], Mohd Zamri Che Wanik [a]

[a] Department of Electrical, Electronic and System Engineering, Faculty of Engineering and Built Environment, Universiti Kebangsaan Malaysia, Bangi 43600, Selangor, Malaysia
[b] Faculty of Electrical and Electronic Engineering, Universiti Malaysia Pahang, Pekan 26600, Malaysia

ARTICLE INFO

Article history:
Received 4 April 2013
Received in revised form 30 December 2013
Accepted 21 March 2014
Available online 18 April 2014

Keywords:
Stability index
Voltage collapse prediction
Distributed generation
Maximum power transfer
Loadability
Voltage variation

ABSTRACT

The Objective: This paper presents a method to identify the optimal location and size of DGs based on the power stability index and particle swarm optimization (PSO) algorithm.
Materials and methods: First, a novel maximum power stability index (MPSI) is derived from the well-established theorem of maximum power transfer. The MPSI is utilized as an objective function to determine the optimal DG locations. Next, a PSO-based model with randomized load is developed to optimize DG sizing in view of the system's real power losses.
Results and Conclusion: Lastly, a IEEE 30-bus test system is employed in the simulation. The performance of proposed MPSI index are comparable with other voltage stability indices. The DG optimization model considering voltage stability and loss minimization provides better results compared to that obtained using only loss minimization approach.

Introduction

A healthy power system should be stable at any time while satisfying various operating criteria. The modern power system is challenged with the increasing load demands from the industrial, commercial and residential sectors [1,2]. The large increase of load demands has caused congestion in transmission lines which further lead to instability the in power system operation [3] .The significance of this phenomenon has increased nowadays as many major blackouts are caused by power system instability [4]. Untreated large and weak networks with recurring voltage variations are inevitably prone to voltage collapse. Thus, maintaining voltage stability is one of the major concerns in power system operation. The enhancement of voltage stability through distributed generation has been widely adopted by utility companies worldwide [5,6].

The promotion of distributed generator (DG) resources in power systems offers benefits, such as reduction in power losses, improvement in voltage profile and reduction of on-peak operating costs. The trend in electricity charge promotes the location and time base pricing schemes. At peak periods, DGs can be used to supply some load demands thus reduce the cost of power taken from the network during high electricity charges [7–9]. The utilization of DG can serve as a hedge against transmission and distribution expansion costs. The on-site electricity generation could result in cost savings in terms of transmission and distribution of about 30% of electricity energy costs [10].

Two major aspects, namely, location and sizing of DG require careful attention. Before discussing several impacts formed by these two factors; is important to have understanding of the meanings. According to [11], the location of DG is clearly defined as the installation and operation of DG units connected directly to the distribution network or on the customer site of the meter. The purpose of DG is to provide a source of active electric power, as such, the capacity to provide reactive power does not need to be included in DG sizing [11]. The definition for DG sizing given by other organizations [12,13] are also in view of active power rating.

Various methods that consider both basic and advanced techniques to solve DG placement and sizing problems were introduced by researchers. Among the conventional optimization methods utilized to predict the allocation of DGs are linear programming, Kalman's filter algorithm, and gradient method [14–16]. Studies have been conducted recently to assist utility companies using advanced and intelligent techniques, such as exhaustive algorithm, tabu search, fuzzy-genetic algorithm, and artificial bee colony algorithm, to fulfill various optimization objectives [17–21].

The optimal DG location and size are determined in this study through the proposed maximum power stability index (MPSI) with particle swarm optimization (PSO) to improve power system stability and reduce active power losses. First, a brief mathematical description of the proposed index is presented as principle for DG

* Corresponding author at: Faculty of Electrical and Electronic Engineering, Universiti Malaysia Pahang, Pekan 26600, Malaysia. Tel.: +6012 387 9320.
E-mail address: ruhaizad@ump.edu.my (R. Ishak).

http://dx.doi.org/10.1016/j.ijepes.2014.03.044
0142-0615/

placement. Then, MPSI and PSO with the continuation power flow are combined to determine the most sensitive load buses to voltage collapse. Lastly, a simulation is conducted on the IEEE 30-bus distribution network with MATLAB to validate the effectiveness of the proposed method. The simulation results indicate that the technique is feasible for practical implementation.

Concept of voltage stability

Static and dynamic

The different methods utilized to assess voltage stability can be broadly classified into two types, namely, dynamic and static methods [22]. Dynamic or time-domain method is useful in understanding the mechanism of voltage collapse and the coordination of protection controls. Static or steady-state analysis is concerned with the assessment of the proximity of the system to a voltage collapse event. The static type of study considers a wide array of system operating conditions, including contingencies such as line outages, loss of generating units, and loss of compensating devices. Voltage stability studies usually involve static analysis.

Voltage collapse events can be caused by many triggering factors, such as load variation, generator control limits, reactive power compensation limits, and malfunctioning voltage control devices. Among the key factors influencing the voltage stability of a power system is load variation or load characteristic. Power systems are expected to become heavily loaded in the future as the demand for electric power increases with the expansion of economic growth.

Load characteristics

Voltage stability concerns with the ability of a power system to maintain acceptable bus voltages under nomal operating condition and after being subjected to a disturbance [23]. Typically the voltage stability problems are analyzed based on estimation of the maximum loadability and the computation of critical power system loading that eventually lead to voltage collapse events [24]. Voltage collapse can easily occur in a heavily loaded power system when the system operates close to the stability limits. With the increasing of load demand, interest in voltage stability studies is often determined by the maximum amount of active power that can be delivered to the end users.

For a simple 2 bus system shown in Fig. 1a, the change in load characteristic affects the voltage, current and active power at the load bus can be illustrated by Fig. 1b. At receiving bus, as the load demand increased, the amount of active power delivered by the system to the bus also increases until it reaches a maximum value. The power transferred reaches the maximum value when the load impedance Z_L is equal to source impedance Z_S. Fig. 1a indicates that point where $Z_L = Z_S = 1$ is the critical loading point for the system to operate satisfactorily. Further increase beyond the critical loading point would adversely cause the system voltage to collapse.

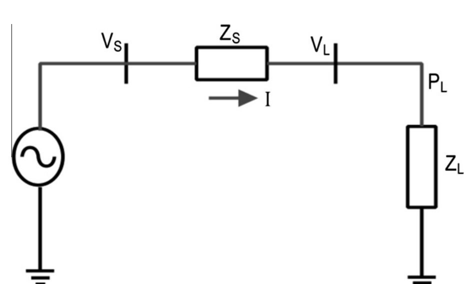

Fig. 1a. 2-Bus system.

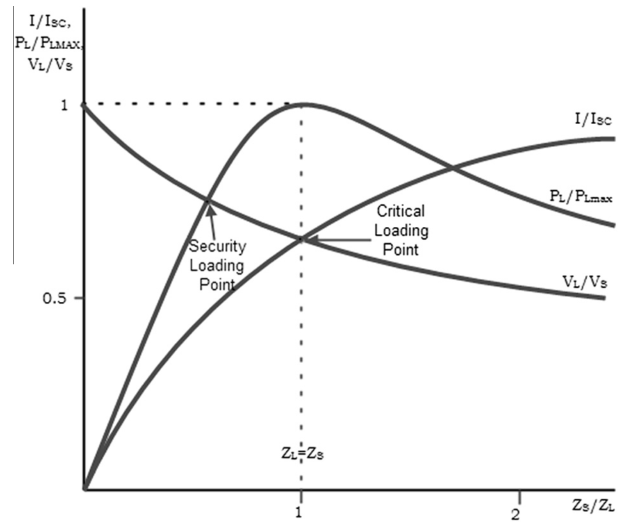

Fig. 1b. Load demand function [25].

Performance index

The main focus in voltage stability studies in power system is the identification of weak or critical buses. Voltage instability in power systems can be analyzed based on P-V and Q-V characteristics. The P-V curve exhibits a function of active power transfer variation with the bus voltage while the Q-V curve shows the sensitivity of bus voltage with respect to reactive power variation.

Each method dictates different advantages that compliments the limitations of another. For instance, the conventional P-V curves have been referred by network operators and industries to predict the *r* point of maximum loadability in a system. The curve is suitably used with peak assessment of highly loaded power system. On the other hand, the Q-V curve highly assists in assessment of reactive power compensators placement or sizing such as static VAr compensators and capacitor banks.

The present load demand scenario shows a large and continuous increment. The use of conventional P-V method for large network stability assessment suffers from exhaustive computational work. Recently researchers have employed the voltage index-based methods [26–29] to obtain fast and reliable results in identifying weak and susceptible buses in the network. In [30], the voltage index-based method is used with DG application.

Formulation of maximum power stability index

Reduced network circuit

The assessment of stability in large networks can be exceptionally demanding task. Model reduction method is often employed to reduce the computational burden. The method transforms a multiple bus network into an equivalent 2-bus Thevenin model. The formulation of MPSI index begins with the transformation of network as shown in Figs. 2a and 2b.

The power flow equation at node *j* in the local network can be written as:

$$V_j[Y_j][V] = S_j \tag{1}$$

where S_j is the apparent load power, V_j is the voltage magnitude at the load bus, $[V]$ contains the nodal voltages; $[V] = \begin{bmatrix} V_1 \\ V_2 \\ .. \\ V_n \end{bmatrix}$.

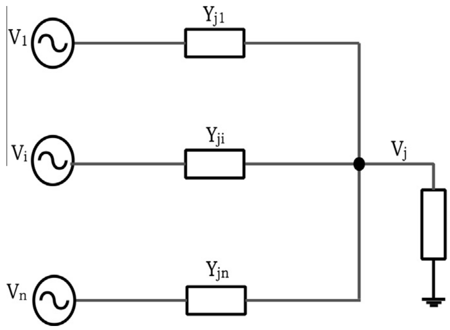

Fig. 2a. Typical local network.

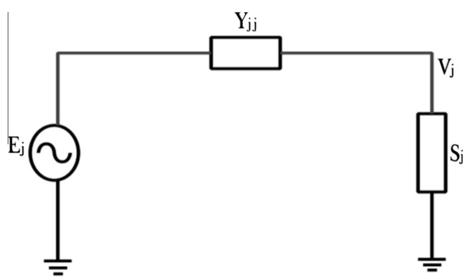

Fig. 2b. Reduced circuit.

In Eq. (1), $[Y_j]$ is row j-th admittance matrix and we can write:

$$[Y_j] = [-Y_{j1} - Y_{j2} - \cdots + Y_{jj} \cdots - Y_{jn}]$$

where Y_{ji} is admittance between node j and node i, $Y_{ji} = G_{ji} + iB_{ji}$ and $i = 1\ldots n$, $i \neq j$, Y_{ji} is self admittance at node j

$$Y_{jj} = \sum\nolimits_{i=1, i\neq j}^{n} Y_{ji}$$

The equivalent voltage of the network E_j obtained from node j can be written as:

$$E_j = \frac{\sum_{i=1, i\neq j}^{n} Y_{ji} V_i}{Y_{jj}} \tag{2}$$

Substituting Eq. (2) for Eq. (1) will give:

$$V_j^* (E_j - V_j) Y_{jj} = S_j^* \tag{3}$$

Eq. (3) is the load flow equation of the reduced network.

Maximum power transfer theorem

The maximum power transfer (MPT) theorem can be applied to ac and dc circuit analysis. The MPT theorem states the maximum power is transferred to a resistive load when the load resistance is equal to the internal resistance of the source in dc analysis. Similarly to ac circuit, the maximum power transfer condition can be achieved when the load impedance Z_L is equal to the source or Thevenin impedance Z_{Th} as shown in Fig. 2b. In ac circuit, the Thevenin impedance Z_{Th} can be written as:

$$Z_{Th} = R_{Th} + jX_{Th} \tag{4}$$

Both resistance and reactance are considered in the equivalent Thevenin impedance calculation. Referring to MPT, the interest is to find the value of load resistance R_L and reactance X_L such that the power absorbed from the source is maximum.

The purpose of developing the new stability index is to be used with DG application. It has been claimed by [11], the inherent role of DG is to be used as a source of active power; such it is not necessary for DG to be able to produce reactive power. With respect to this definition, the derivation of the proposed voltage stability index focuses on the active power delivery in a network. The idea of maximum power transfer is to maximize the amount of active power that can be delivered to the load.

From Fig. 1a, the active power P_L at the load can be written as:

$$\begin{aligned} P_L &= \widetilde{V}_L \widetilde{I}_L \cos\theta \\ &= Re(V_L I_L^*) = \tfrac{V_L^2}{ReZ_L} \end{aligned} \tag{5}$$

Assuming that voltage and impedance of the source are priorly known; therefore, the real power expression P_L can be restated in terms of voltage and impedance of the source as:

$$P_L = Re(V_L I_L^*). \tag{6}$$

where

$$V_L = \frac{Z_L}{Z_{Th} + Z_L} V_{Th} \tag{7}$$

and

$$I_L^* = \left(\frac{V_{Th}}{Z_{Th} + Z_L}\right)^* \tag{8}$$

The complex load power S_L can be written as:

$$\begin{aligned} S_L &= V_L I_L^* \\ &= \tfrac{V_{Th}^2}{|Z_{Th}+Z_L|^2} Z_L. \end{aligned} \tag{9}$$

Thus, the active power P_L can also be expressed as:

$$\begin{aligned} P_L &= Re(V_L I_L^*) \\ &= Re\left(\tfrac{V_{Th}^2}{|Z_{Th}+Z_L|^2} Z_L\right) Re(Z_L) \\ &= \tfrac{V_{Th}^2 R_L}{(R_{Th}+R_L)^2 + (X_{Th}+X_L)^2}. \end{aligned} \tag{10}$$

From [31], the delivered active power P_L is maximized when $R_L = R_{Th}$ and $X_L = -X_{Th}$, the load impedance is equal to the complex conjugate from Thevenin impedance.

Thus, the maximum real power absorbed by the load P_{Lmax} is:

$$P_{Lmax} = \frac{V_S^2 R_L}{(R_L + R_L)^2 + (-X_L + X_L)^2} = \frac{V_{Th}^2}{4R_L}. \tag{11}$$

According to theory of voltage stability, there is a maximum limit of power that can be transferred by the network. In [25] pointed out that maximum active power transfer is obtained when $Z_L/Z_{Th} = 1$. The condition represents critical loading point that must be avoided to preserve stability. The plot of power versus load in Fig. 1b shows that when the load demand increases, the receiving power also increased until it reaches the maximum transfer limit.

At the point where Z_L/Z_{Th} =1, the ratio of P_L to P_{Lmax} also shows unity value.

$$\frac{P_L}{P_{Lmax}} = 1 \tag{12}$$

By substitute P_L from Eq. (5) and P_{Lmax} from Eq. (11) into power ratio expression in Eq. (12) leads to the formulation of the proposed voltage stability index:

$$MPSI = \frac{4V_L^2}{\left[\frac{\sum_{i=1,i\neq j}^{n} Y_{ji} V_i}{Y_{jj}}\right]^2} \tag{13}$$

Eq. (12) defines the collapse criterion of the index. Any value close to 0 represents stable operating condition in contrary any value close to 1 implies critical operating condition.

Index performance

To verify the validity of the proposed index, the MPSI is tested with other known voltage stability indices that are power transfer stability index PTSI [32] and voltage collapse prediction index VCPI [33]. The formulation of PTSI is based on derivative of maximum load apparent power with respect to load impedance change while the formulation of VCPI is based on determinant evaluation of partial derivative matrix in Newton Raphson power flow. Both indices will give value close to 0 under stable operating condition whereas unstable condition leading to voltage collapse will show value close to 1.

There are many aspects that can be selected to verify the sensitivity of an index in measuring bus proximity to voltage collapse. It is known that voltage drop in power system is greatly influenced by the load demand. Thus, in this work, the performance of the index is tested with respect to load changes. By increasing the load demands, system voltage level will eventually pull towards the critical point.

For this test, the loading is progressively increased until the voltage drops below the 0.9 p.u. level. When bus voltage drops below this limit, the voltage at the bus is likely to collapse and cause divergence in Newton–Raphson load flow solution.

Proposed DG placement and sizing algorithm

Particle swarm optimization (PSO)

Kennedy and Eberhart proposed PSO in 1995 as one of the evolutionary computation algorithms based on a social–psychological metaphor [34,35]. A population of individuals referred to as particles adapts by returning stochastically toward previously successful regions. Two primary operators exist in this method, namely, position update and velocity update. Each particle during each generation is accelerated toward the particle's previous best position and the global best position. The new velocity in each iteration for each particle is referred to as current velocity, which is the distance from the previous best position and global best position. The value of the new velocity is utilized to compute the next position of the particle in the search space. This process is iterated a number of times until the lowest error is obtained. The particle position in dimensional space is illustrated in Fig. 3.

Let X_i^k be the current position of agent i or particle i at iteration k, where

$$X_i = (X_{i1}, X_{i2}, X_{i3} \ldots X_{in}) \tag{14}$$

and V_i^k is the current velocity of particle i at iteration k, where:

$$V_i = (V_{i1}, V_{i2}, V_{i3} \ldots V_{in}) \tag{15}$$

The local best position related to the lowest value (for minimization) of the objective function for each particle is denoted as:

$$P_{best_i} = (P_{best_{i1}}, P_{best_{i2}}, P_{best_{i3}} \ldots P_{best_{in}}) \tag{16}$$

while the global best position among all the particles or the best P_{best} is denoted as:

$$G_{best_i} = (G_{best_{i1}}, G_{best_{i2}}, G_{best_{i3}} \ldots G_{best_{in}}) \tag{17}$$

The particle new velocity and position are determined by following equations respectively:

$$V_i^{k+1} = c0 * v_i^k + \frac{c1 * r1\left(P_{best_i}^k - X_i^k\right)}{\Delta t} + \frac{c2 * r2\left(G_{best_i}^k - X_i^k\right)}{\Delta t} \tag{18}$$

$$X_i^{k+1} = X_i^k + \Delta t * v_i^{k+1} \tag{19}$$

where $i = 1, 2, \ldots n$ is the number of dimensions for each particle; $c1$ and $c2$ are the constants of acceleration; k is the number of times of iteration; Δt is the time step for each iteration; $r1$ and $r2$ are two random numbers within the range of [0,1]; and $c0$ is the inertia weighting factor.

Optimal DG placement

The DG placement problem is a nonlinear constrained optimization problem. The proposed solving algorithm is divided into two sub-problems. The first sub-problem is where the optimum DG location is identified through a voltage stability assessment method. The goal is to add DG at the weakest bus in the system as the load demand randomly increased. The optimum location can be quickly identified using the proposed index. In this study, DGs are considered operating at unity power factor to support the system peak demand.

Optimal DG sizing

Although DG is a relatively new concept but a variety of optimization techniques have been developed by researchers. From literature, the evaluation of optimal DG size as a function of power losses have always captured researchers concern. The second sub-problem in this work, which is the sizing of DG has also considered the minimization of active power losses.

In selecting the capacity of DG, the size of load delivery area is important. According to [11,36,37] there is no agreement on the maximum capacity of DG. However [19] suggested the best size of DG such that it is consumable locally without the intention of exporting the energy beyond the substation boundary. The intention of exporting the energy will lead to very high losses. The reason for high losses with high capacity of DG can be explained from Fig. 4.

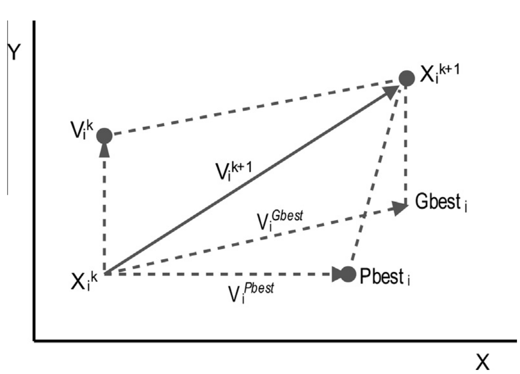

Fig. 3. PSO point search.

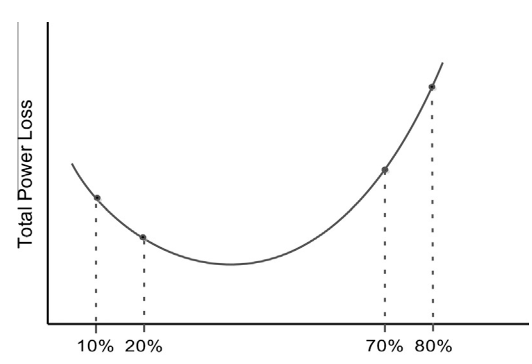

Fig. 4. Power loss with load demand.

The relation between total power loss and total demand is represented by quadratic function. The left part of the curve shows that power loss reduction decreased proportionately with the injected power by DG. The DG obtained its optimum capacity when the power loss of the system has reached the minimum value as represented by the lowest point on the curve.

During instance of high power added from DG (right part of the curve), the minimum losses value is exceeded and losses start to increase. This is due to excess currents from the DG flow into adjacent buses causing increase in transmission losses.

Apart from this, it also seems appropriate to put a limit to DG capacity so as to keep the concept of DG, a small distributed generation and not a large centralized generation plant.

Simulation procedure

The flowchart of the proposed method is shown in Fig. 5. The major steps are summarized as follows:

Step 1: A set of system loading cases (real and reactive power loadings) is generated by the PSO algorithm because the major interest in voltage stability assessment is to determine the bus voltage when the load increases.
Step 2: A continual load flow is launched for each loading case generated in Step 1, and the MPSI index for each bus is calculated to identify the weak buses in the system.
Step 3: The fitness function for each bus is evaluated by Eq. (18). The best particle with the highest value of MPSI represents the optimal DG location. The formulation for index maximization is provided by:

$$G = \text{Max MPSI}(i) \quad \text{for } i = 1, 2 \ldots, n_b \tag{20}$$

where n_b is the number of load buses

Subject to

$$V_i^{min} \le V_i \le V_i^{max}$$

Step 4: A set of DG sizes that consider real and reactive power loads is generated again through PSO based on the optimal DG location obtained in Step 3.
Step 5: Power flow is launched for each DG size generated in Step 4. The fitness function is evaluated for total power loss in the system, which provides the current P_{best} for the optimal DG size. The mathematical formulation for loss minimization is provided by Eq. (19).

$$f = \text{Min} \sum_{x=1}^{n} P_{loss}(x) \tag{21}$$

$$\text{Subject to} \quad V_i^{min} \le V_i \le V_i^{max}$$
$$P_{DG}^{min} \le P_{DG} \le P_{DG}^{max}$$

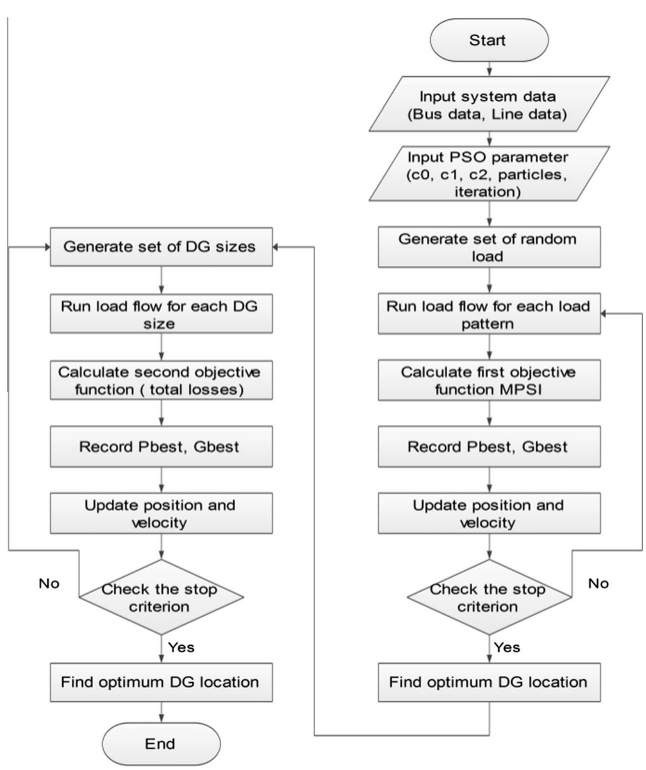

Fig. 5. Flowchart of the proposed algorithm.

Simulation results and discussion

The proposed method was tested on IEEE 30-bus test system with total load 283.4 MW. The system consists of 24 load buses, 6 generator buses, and 41 transmission lines [38] as shown in Fig. 6. For simulation, the system load is randomly varied between 0% to 25% above the base case to simulate the increasing load demand scenario.

Validation of voltage stability index

The aim of this simulation is to have a performance comparison between the three different indices in selecting sensitive or weak buses in the test system. The critical buses in the system is studied with respect to load increasing contingency. Considering that contingency may possibly happen at any location in the system, bus 17 centrally located in network is selected as the contingency bus.

The voltage at three load buses i.e. bus 7, 15 and 26 are monitored and their index values are calculated a for each loading case. The index calculation for bus 7, 15 and 26 under increasing load change is presented in Table 1. As mentioned earlier, all three indices will show value close to 1 when voltage stability in the system decreased.

From the results, index VCPI changed a little with the increase in load. Meanwhile index PTSI relatively shows larger increase

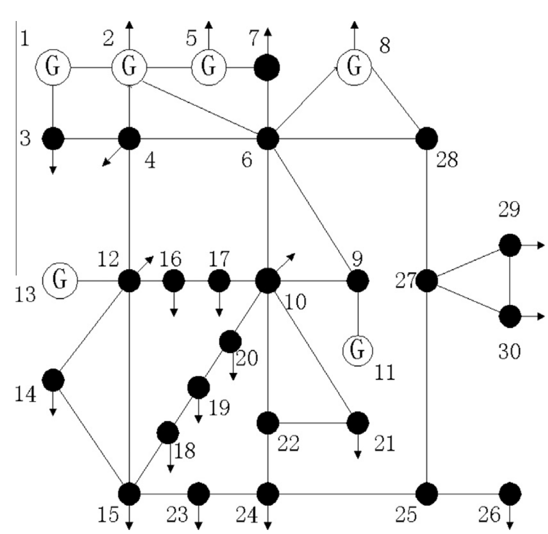

Fig. 6. IEEE 30-bus test system.

Table 1
Voltage stability index with load increment.

Load increment (%)	MPSI			PTSI			VCPI		
	Bus 7	Bus 15	Bus 26	Bus 7	Bus 15	Bus 26	Bus 7	Bus 15	Bus 26
105	0.0843	0.1590	0.2348	0.0708	0.0986	0.1887	0.0584	0.0713	0.1201
110	0.0915	0.1823	0.2622	0.0937	0.1240	0.2109	0.0773	0.0925	0.1374
115	0.1496	0.2212	0.3156	0.1429	0.1794	0.3129	0.1017	0.1419	0.2016
120	0.1989	0.2648	0.3973	0.2051	0.2567	0.3353	0.1318	0.2098	0.2128
125	0.2714	0.3425	0.4805	0.2697	0.3219	0.4283	0.1675	0.2480	0.2795
130	0.3377	0.4152	0.5639	0.3091	0.3709	0.4933	0.1941	0.2723	0.3216
135	0.3765	0.4818	0.6910	0.3278	0.4482	0.6513	0.2083	0.3051	0.4136
140	0.4629	0.6073	0.8017	0.3869	0.5435	0.7325	0.2337	0.3592	0.4781
145	0.4809	0.6891	0.9121	0.4057	0.6098	0.8872	0.2798	0.3944	0.5503
150	0.5150	0.7141	1	0.4196	0.6427	0.9849	0.2925	0.4178	0.5939
160	0.5413	0.7565	1	0.4372	0.6891	1	0.3382	0.4366	0.6503

however the linear in load increment pattern implies non-linear characteristic in the index. In this case, the value calculated by MPSI offers a good indication about the proximity to voltage collapse. Index MPSI shows stable variation in proportion to load increment thus the index can be used to accurately predict voltage stability in power systems.

Impact of DG on voltage profile

An analysis is conducted to study the impact of non-optimal DG location on system voltage profile. For this, the system bus voltage is monitored from the load flow before and after the integration of DG. The bus voltage and power margin has interrelated function. Using P-V analysis method, the function of system voltage stability with active power margin can be determined.

The effect of DG on bus voltage can be explained with simple illustration of P-V curve as shown in Fig. 7. The installation of DG on a particular bus, will increase the active power margin of the bus by ΔP. At the same time, it can be seen that the bus operating voltage will move from present V_0 to new V_{DG}. As a result, the voltage level at that bus will increase. Thus, proper allocation of DG in a distribution system will help improve the voltage level and stabilize the system operation.

In this analysis, the active power margin at load bus is determined by increasing the loading of the bus gradually until the load flow diverges.

Since the purpose of this analysis is to see impact of non-optimal DG location on voltage profile; it is not necessary to find the power margin for each bus in the system. Basically the buses are selected based on its loading characteristics and distance from neighboring buses. The margin is calculated by assuming the voltage limit 0.95 p.u. is respected for each bus. The calculated active power margin of the load buses is in Fig. 8.

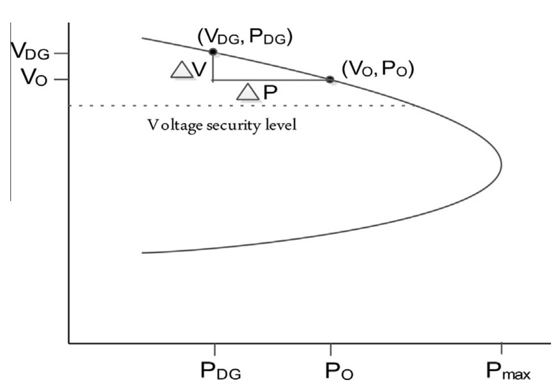

Fig. 7. P-V curve with DG.

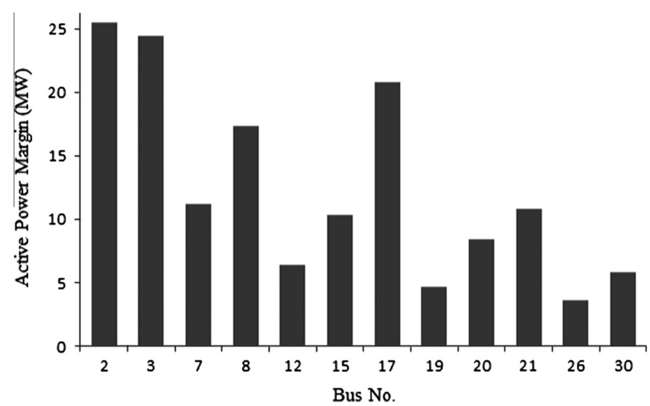

Fig. 8. Active power margin of the system.

It can be observed that bus 26 has the lowest power margin, which represents the weakest bus in this system while bus 2 is the highest, is the strongest bus. Assume an arbitrary 5 MW DG is connected to supply constant active power the system. Placing the DG on the most weak and strong bus will give significant impact on system voltage profile. The results are shown in Fig. 9 when DG is installed at extremely weak and strong buses in the system. The figure shows when DG is installed at bus 2, the voltage level at bus 2 increased above 1.0 p.u while at the same time voltage at bus 26 drops slightly below the critical level. The results clearly demonstrates the impact when DG is located at non-optimal location.

Impact of DG on power losses

In order to verify the effect of optimal DG sizing on power system operation, an analytical test showing the variations of active power loss relative to DG injection at each bus is carried out. The total active power loss in the system is evaluated in three different cases:

(1) Case 1: 2 MW DG unit is added.
(2) Case 2: 4-MW DG unit is added.
(3) Case 3: 6-MW DG unit is added.

In each case, the DG is added sequentially and the power flow analysis is carried out to find the total power loss in the system. Similar step is repeated for case 2 and 3 for with respective DG sizes. In Case 1, from Fig. 10 it can be observed that as 2-MW DG is added in bus 15, 17, 18, 26 and 30, the active power losses in the system has reached the lowest reduction in the range between 32.3 to 32.7 MW.

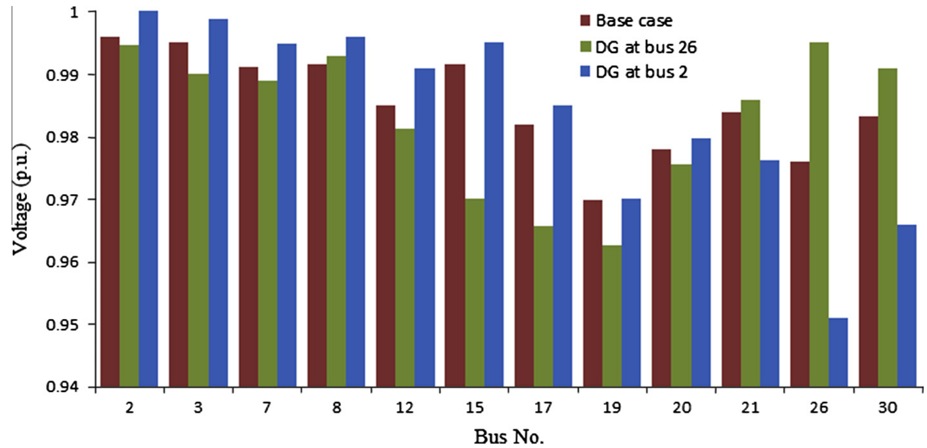

Fig. 9. System voltage for DG located at most weak and strong bus.

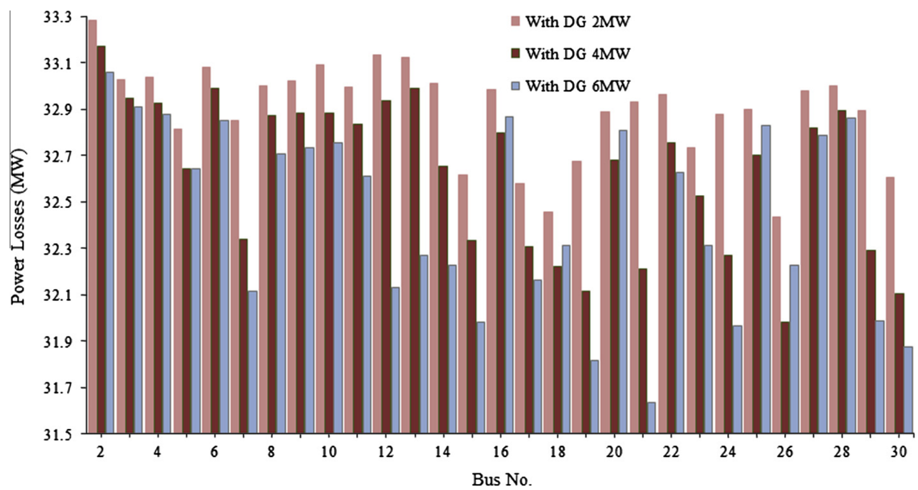

Fig. 10. Power losses for IEEE 30-bus system with different DG sizes.

In Case 2, again the active power loss is evaluated when a 4-MW DG is placed at different buses in the system. Case 2 is expected to be better than Case 1 due to larger capacity of DG. In practice, installing large DG incurs high investment costs; utilities or energy providers may consider to add only few DGs to the system. Therefore is important to identify optimal location in which the total power loss is truly minimum. Considering single DG placement for Case 2, indicated in Fig. 10 the total active power loss reaches minimum value around 32 MW when the DG is located at bus 26. The losses with DG at bus 26 significantly preceded the losses recorded at other buses.

The observations produced by Case 3 are much interesting to be analyzed. With a 6-MW DG added to the system; from logical sense it can be anticipated the results are much better than the previous two cases. However, it is found that the active power losses at bus 26 as shown in Fig. 10 has increased slightly. Since the load demand in bus 26 remains unchanged at 9.91 MW, the unconsumed amount of active power supplied by the DG flows into the network cause an increase in power losses. The quadratic power loss effect can also be observed at bus 16, 18, 20 and 25; however, the severity is less. The reason is due to shorter length for the excess power to be transfer to other load buses.

On another note, when the 6-MW DG is placed at bus 19, 21, 24, 29 and 30, the active power losses in the system effectively reduced to more than 32 MW. The system achieves minimum power losses of about 31.6 MW when DG is located at bus 21. The amount of reduction in these buses surpassed the maximum losses reduction recorded at bus 26 in Case 2.

A common practice with DG installation plan is to make the best use of its presence. Given the scenario in Case 3, utilities may opt to another solution by partitioning the DG capacity into smaller sizes with the intention to maximize the power losses reduction. Using the same approach, a lengthy analysis is required to find the appropriate solutions. Evaluation of power losses with one DG at a time at each bus requires several power flow solutions. More than that, computation time will increase proportional to number of buses. As such, the heuristic optimization method employed in this work can provide a quick solution for the optimal sizing of DG with good accuracy.

Further discussion on the findings of the proposed sizing method for two DG units is given in Section 5.5.

Optimal one DG unit

The result shown in Table 2 represents the bus index upon execution of the proposed algorithm. The potential locations where the DG can be installed are buses 18, 19, 21, 26, and 30. Maximization of the MPSI index with respect to voltage limit indicates that bus 26 is the optimal location for DG placement. Fig. 6 shows that bus 26 is located at large distance from the generators. Thus, bus 26 is largely affected by load variation in the system.

Table 2
Bus index for first DG.

Bus No.	MPSI Index		
	Case1	Case2	Case3
3	0.1995	0.1977	0.2024
4	0.1719	0.1704	0.1745
6	0.1654	0.1639	0.1679
7	0.2253	0.2232	0.2287
9	0.1845	0.1828	0.1873
10	0.2637	0.2613	0.2677
12	0.2558	0.2535	0.2596
14	0.2830	0.2805	0.2872
15	0.2791	0.2766	0.2833
16	0.3175	0.3146	0.3223
17	0.3496	0.3465	0.3549
18	**0.4210**	**0.4172**	**0.4273**
19	**0.3972**	**0.3936**	**0.4032**
20	0.3433	0.3402	0.3484
21	**0.3781**	**0.3747**	**0.3838**
22	0.2936	0.2910	0.2980
23	0.3147	0.3119	0.3194
24	0.3299	0.3269	0.3348
25	0.2676	0.2652	0.2716
26	**0.5113**	**0.5067**	**0.5190**
27	0.2079	0.2060	0.2110
28	0.1994	0.1976	0.2024
29	0.2956	0.2929	0.3000
30	**0.3624**	**0.3591**	**0.3678**

Bold values are represent five critical cases of each measurement.

Table 3
Bus index for second DG.

Bus No.	MPSI Index		
	Case1	Case2	Case3
3	0.0275	0.0268	0.0281
4	0.0381	0.0371	0.0388
6	0.0162	0.0158	0.0165
7	0.0659	0.0642	0.0672
9	0.0087	0.0085	0.0089
10	0.0535	0.0521	0.0546
12	0.1726	0.1681	0.1761
14	0.2254	0.2195	0.2299
15	0.1934	0.1884	0.1973
16	0.2011	0.1959	0.2051
17	**0.2784**	**0.2712**	**0.2840**
18	0.2272	0.2213	0.2317
19	**0.2809**	**0.2736**	**0.2865**
20	**0.2620**	**0.2552**	**0.2672**
21	**0.2558**	**0.2491**	**0.2609**
22	0.1932	0.1882	0.1971
23	**0.2727**	**0.2656**	**0.2782**
24	0.2025	0.1972	0.2066
25	0.1213	0.1181	0.1237
26	0.1938	0.1888	0.1977
27	0.0473	0.0460	0.0482
28	0.0329	0.0320	0.0336
29	0.1266	0.1233	0.1291
30	0.2056	0.2003	0.2097

Bold values are represent five critical cases of each measurement.

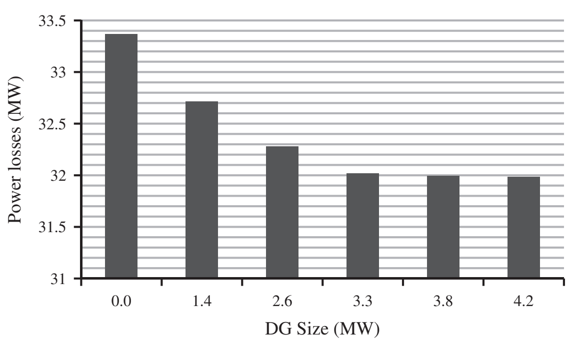

Fig. 11. Power losses with one DG unit.

The optimal DG size for bus 26 is calculated with random loading. The optimization algorithm adjusts the suitable DG size by minimizing the total active power losses in the system. Fig. 11 shows that minimum power loss achieved when the size of the DG is equal to 3.3 MW. The injection of active power from the DG reduces the power losses in the network. However, further increase in injection size renders the loss reduction insignificant.

The voltage profile for the system before and after DG installation is given in Fig. 12. It can be observed from the figure that bus 26 has the lowest voltage level i.e. 0.90 p.u. without DG. The support from 3.3 MW DG unit on the bus has increased the voltage above the critical limit.

Optimal two DG units

The voltage profile curve can be further improved by installing more DGs in the system. This section considers the installation of two DG units with optimum location and size. The search for the second DG location commences after the first unit is successfully installed in bus 26. As shown in Table 3 bus 19 shows the greatest voltage reduction at peak loading thus the most weak among the five potential buses. Bus 19 is considered the most suitable for second DG location.

To find the optimal size of DG at bus 19, again optimal power flow program is executed to minimize power losses. The algorithm gives a solution by repeatedly allocates different DG sizes that fits the objective function. Size is fixed when the amount of power loss is minimum. The result indicates that two units of DGs, each rating

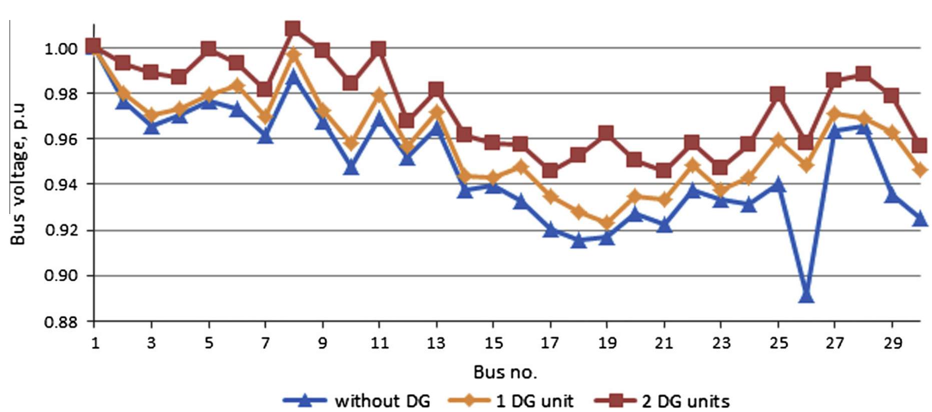

Fig. 12. Voltage profile for IEEE 30-bus with DG.

Table 4
Power loss reduction.

Case	DG location (bus)	DG size (MW)	Total size (MW)	Power loss (MW)	Power loss reduction (%)
Base	N/A	N/A	N/A	33.368	N/A
1	26	3.3	3.3	32.018	4.05
2	19	2.9	6.2	31.197	6.51
	26	3.3			

2.7 MW and 3.3 MW; placed at bus 19 and 26 respectively, has further reduced the power losses obtained in Case 1 by 2.5% as shown in Table 4.

The system shows minimum power loss of 31.197 MW when DGs are installed at bus 19 and 26 totalling capacity 6.2 MW. Although the capacity is slightly different than the capacity of DG used in Case 3 of Section 5.2 but the difference is small compared to the amount of losses reduced. Without loosing much accuracy, it can be assumed negligible and consider taking up the same value if rounded off. Other than that, the voltage profile in the system with two DGs also shows better result as shown in Fig. 12.

Comparison of methods

In this section, the results of the proposed method has been compared with other optimization methods by [39–41] for IEEE 30-bus system. Table 5 shows the comparison of percentage real power loss reduction (PLR) with DG. PLR is the ratio of active power losses reduction with DG to active power losses without DG in the base case.

The optimized penetration level (PL) represents the total capacity of DG installed at optimal locations. The penetration level (PL) of DG in power system is calculated by:

$$Penetration\ level(\%) = \frac{P_{DG}}{P_{Load}} * 100\% \tag{22}$$

The base case load without DG for all methods are same. For one unit DG, a substantial reduction in total system real power, approximately 31% is obtained by method 2 when DG is placed at bus 30. It is observed that method 3 and 1, each losses reduction is about 11.3% and 7.7% while the proposed method has the lowest losses reduction around 4.1%.

However considering the amount of power losses reduced with the level of DG penetration in this system, will give a different perspective overall. The amount of DG penetration in method 2 is 16.67 times higher than the proposed method. The effectiveness of DG contribution against power losses can be quantified by dividing PLR over PL. As a result, the proposed method shows the highest effectiveness followed by method 3 while method 1 and 2 are equally same.

Table 5
Comparison with different methods for DG optimization.

Method	1 DG unit			2 DG units		
	Weak bus	PL (%)	PLR (%)	Weak buses	PL (%)	PLR (%)
Method 1 [39]	5	5	7.7	-nil	-nil	-nil
Method 2 [40]	30	20	30.93	7.29	20	30.65
Method 3 [41]	5	3.49	11.29	5.21	5.78	16.51
Proposed method	26	1.2	4.05	19.26	2.2	6.5

Optimizing for 2 units of DG, method 1 does not include. Method 2 considers completely different buses for both locations whereas other two remains the location of first DG unit. For the proposed and method 3, further reduction in system power losses i.e. 6.5% and 16.5% are recorded respectively. As shown however method 2 slightly increased. Again taking into account the effectiveness of each MW power of DG contribution towards power loss reduction, the proposed method shows the best performance. The proposed DG optimization method using voltage stability index MPSI and active power loss minimization with PSO can give promising results.

Conclusion

In this study, the optimum DG location and size for improved voltage stability is determined through the proposed MPSI index and power loss minimization technique. Maximum power stability index is a fast and reliable tool to analyze the state of voltage stability in power system. The index is used to identify weak buses that allow only small load variations in the system. The critical buses which represent optimum DG locations are identified using PSO search algorithm.

The optimum DG size is evaluated based on the second objective function which minimizes the total active power loss. The simulation results indicated that the overall impact of the DG units on voltage stability is positive and proportionate reduction in power losses is achieved.

Acknowledgements

This work was supported by Ministry of Higher Education, Malaysia (MOHE) under the SLAI programme and jointly carried out by Faculty of Engineering and Built Environment, Universiti Kebangsaan Malaysia and Faculty of Electrical & Electronics Engineering, Universiti Malaysia Pahang.

References

[1] Singh D, Singh D, Verma KS. Multiobjective optimization for DG planning with load models. IEEE Trans Power Syst 2009;24(1):427–36.
[2] Jamian JJ, Aman MM, Mustafa MW, Jasmon GB, Mokhlis H, Bakar AHA. Comparative study on optimum DG placement for distribution network. Przegląd Elektrotechniczny 2013;89(3A):199–205.
[3] Vijayakumar K, Jegatheesan R. Optimal location and sizing of DG for congestion management in deregulated power systems. In: Swarm, evolutionary, and memetic computing. Berlin Heidelberg: Springer; 2012. p. 679–86.
[4] Guedes RBL, Alberto LFC, Bretas NG. Power system low-voltage solutions using an auxiliary gradient system for voltage collapse purposes. IEEE Trans Power Syst 2005;20(3):1528–37.
[5] Joos G, Ooi BT, Mcgillis D, Galiana FD, Marceau R. The potential of distributed generation to provide ancillary services. Proc. IEEE PES Summer Meeting, Seattle, USA. 2000;3:1762–7.
[6] Vovos PN, Kiprakis AE, Wallace AR, Harrison GP. Centralized and distributed voltage control: impact on distributed generation penetration. IEEE Trans Power Syst 2007;22(1):476–83.
[7] Coles L, Beck RW. Distributed generation can provide an appropriate customer price response to help fix wholesale price volatility. IEEE Power Eng Soc Winter Meet 2001;1:141–3.
[8] Sotkiewicz PM, Vignolo JM. Allocation of fixed costs in distribution networks with distributed generation. IEEE Trans Power Syst 2006;21(2):639–52.
[9] Sotkiewicz PM, Vignolo JM. Towards a cost causation-based tariff for distribution networks with DG. IEEE T Power Syst 2007;22(3):1051–60.
[10] Fraser P. Distributed generation in liberalised electricity markets. In: International symposium on distributed generation: power system and market aspects; 2002. p. 1G-12.
[11] Ackermann T, Andersson G, Söder L. Distributed generation: a definition. Electr Power Syst Res 2001;57:195–204.
[12] Electric Power Research Institute (US). 2013. <http://www.epri.com/gg/newgen/disgen/index.html>.
[13] Cardell J, Tabors R. Operation and control in a competitive market: distributed generation in a restructured industry. J Energy 1998;18(Special Issue):111–36.

[14] Hernándeza JC, Medina A, Jurado F. Optimal allocation and sizing for profitability and voltage enhancement of PV systems on feeders. Renew Energy 2007;32(10):1768–89.
[15] Lee SH, Park JW. Selection of optimal location and size of multiple distributed generations by using Kalman filter algorithm. IEEE Trans Power Syst 2009;24(3):1393–400.
[16] Kumar A, Gao W. Optimal distributed generation location using mixed integer non-linear programming in hybrid electricity markets. IET Gen Trans Dist 2010;4(2):281–98.
[17] Nara K, Hayashi Y, Ikeda K, Ashizawa, T. Application of Tabu search to optimal placement of distributed generators. In: IEEE Power Eng Soc Winter Meeting, vol. 228, 2001. p. 918–23.
[18] Kim KH, Lee YJ. Rhee SB, Lee SK, You SK. Dispersed generator placement using fuzzy-GA in distribution systems. In: IEEE power engineering society summer meeting, vol. 3, 2002. p. 1148–53.
[19] Acharya N, Mahat P, Mithulananthan N. An analytical approach for DG allocation in primary distribution network. Int J Electr Power Energy Syst 2006;28(10):669–78.
[20] Prommee W, Ongsakul W. Optimal multi-distributed generation placement by adaptive weight particle swarm optimization. ICCAS Contr Auto Syst 2008:1663–8.
[21] Lalitha MP, Reddy NS, Reddy VV. Optimal DG placement for maximum loss reduction in radial distribution system using ABC Algorithm. Int J Rev Comp 2009:44–52.
[22] Gao B, Morison GK, Kundur P. Voltage stability evaluation using modal analysis. IEEE T Power Syst 1992;7(4):1529–42.
[23] Kundur P. Power system stability and control. Tata McGraw-Hill Education; 1994.
[24] Hedayati H, Nabaviniaki SA, Akbarimajd A. A method for placement of DG units in distribution networks. IEEE Trans Power Deliver 2008;23(3):1620–8.
[25] Chebbo AM, Irving MR, Sterling MJH. Voltage collapse proximity indicator: behaviour and implications. In: Generation, transmission and distribution, IEE proceedings C, vol. 139(3). 1992. p. 241–52.
[26] Gong Y, Schulz N, Guzman A. Synchrophasor-based real-time voltage stability index. Power Syst Conf Exposit 2006; 1029–36.
[27] Kataoka Y, Watanabe M, Iwamoto S. A new voltage stability index considering voltage limits. Power Syst Conf Exposit 2006;2006:1878–83.
[28] Balamourougan V, Sidhu TS, Sachdev MS. Technique for online prediction of voltage collapse. IEE Proc Gen Trans Distr 2004;4(151):453–60.
[29] Su Y, Wang X. A method for voltage stability assessment based on wide area measurement system. In: Proceedings of the inter. conference power energy eng. Wuhan; 2009. p. 1–4.
[30] Aman MM, Jasmon GB, Mokhlis H, Bakar AHA. Optimal placement and sizing of a DG based on a new power stability index and line losses. Int J Electri Power Energy Syst 2012;43(1):1296–304.
[31] Cartwright KV. Non-calculus derivation of the maximum power transfer theorem. Tech Interface 2008;8(2):1–19.
[32] Nizam M, Mohamed A, Hussain A. Performance evaluation of voltage stability indices for dynamic voltage collapse prediction. J Appl Sci 2006;6(5):1104–13.
[33] Balamourougan V, Sidhu TS, Sachdev MS. Technique for online prediction of voltage collapse. In: IEE proceedings of gen trans dist, vol. 151(4), 2004. p. 453–60.
[34] Eberhart R, Kennedy J. A new optimizer using particle swarm theory. In: IEEE proceedings of the sixth international symposium on micro machine and human science; 1995. p. 39–43.
[35] Kennedy J. The particle swarm: Social adaptation of knowledge. In: Proceedings of the International Conference on Evolutionary Computation. 1997:303–8.
[36] El-Khattam W, Salama MMA. Distributed generation technologies, definitions and benefits. Electric Power Syst Res 2004;71(2):119–28.
[37] Pepermans G, Driesen J, Haeseldonckx D, Belmans R, D'haeseleer W. Distributed generation: definition, benefits and issues. Energy Policy 2005;33(6):787–98.
[38] Yokoyama R, Bae SH, Morita T, Sasaki H. Multiobjective optimal generation dispatch based on probability security criteria. IEEE Trans Power Syst 1988;3:317–24.
[39] Wang C, Nehrir MH. Analytical approaches for optimal placement of distributed generation sources in power systems. IEEE Trans Power Syst 2004;19(4):2068–76.
[40] Raj PADV, Senthilkumar S, Raja J, Ravichandran S, Palanivelu TG. Optimization of distributed generation capacity for line loss reduction and voltage profile improvement using PSO. Elektrika J Electr Eng 2008;10(2):41–8.
[41] Reddy SC, Prasad PVN, Laxmi AJ. Reliability improvement of distribution system by optimal placement of DGs using PSO and neural network. In: IEEE international conference on computing, electronics and electrical technologies; 2012. p. 156–62.